Chinese Chemical Letters 33 (2022) 1584–1588

Contents lists available at ScienceDirect

Chinese Chemical Letters

journal homepage: www.elsevier.com/locate/cclet

Endogenous peroxynitrite activated fluorescent probe for revealing anti-tuberculosis drug induced hepatotoxicity

Nannan Wang[a,1], Han Wang[a,1], Jian Zhang[a,*], Xin Ji[b], Huihui Su[a], Jinying Liu[a], Jiamin Wang[c,*], Weili Zhao[a,b,*]

[a] Key Laboratory for Special Functional Materials of Ministry of Education, School of Materials Science and Engineering, Henan University, Kaifeng 475004, China
[b] School of Pharmacy, Institutes of Integrative Medicine, Fudan University, Shanghai 201203, China
[c] Key Laboratory of Natural Medicine and Immuno-Engineering of Henan Province, Henan University, Kaifeng 475004, China

ARTICLE INFO

Article history:
Received 27 June 2021
Revised 12 September 2021
Accepted 13 September 2021
Available online 17 September 2021

Keywords:
Anti-tuberculosis drug induced liver injury
Peroxynitrite
Fluorescent probe
Drug-induced liver injury
Bioimaging

ABSTRACT

Pyrazinamide (PZA), isoniazid (INH) and rifampicin (RFP) are all commonly used anti-tuberculosis drugs in clinical practice, and long-term medication may cause severe liver damage and toxicity. The level of peroxynitrite ($ONOO^-$) generated in liver has long been regarded as a biomarker for the prediction and measurement of drug-induced liver injury (DILI). In this article, we constructed a BODIPY-based fluorescent probe (**BDP-Py$^+$**) that enabled quickly and sensitively detect and image $ONOO^-$ *in vivo*. Utilizing this probe, we demonstrated the change of $ONOO^-$ content in cells and mice model of DILI induced by acetaminophen (APAP), and for the first time revealed the mechanism of liver injury induced by anti-tuberculosis drug PZA. Moreover, **BDP-Py$^+$** could be applied to screen out and evaluate the hepatotoxicity of different anti-tuberculosis drugs. Comparing with the existing serum enzymes detection and H&E staining, the probe could achieve early diagnosis of DILI before solid lesions in liver *via* monitoring the up-regulation of $ONOO^-$ levels. Collectively, this work will promote the understanding of the pathogenesis of anti-tuberculosis drug induced liver injury (ATB-DILI), and provide a powerful tool for the early diagnosis and treatment of DILI.

Drug-induced liver injury (DILI) is an acute liver disease that can lead to liver failure [1]. Most of the drugs that need to be taken long-termly can cause liver damage. Tuberculosis has become a growing global public health problem because of its long treatment cycle and difficult to cure [2]. Pyrazinamide (PZA), isoniazid (INH), and rifampicin (RFP) as the main prescribed medicines are widely used for the therapy of tuberculosis, which are always required to take orally for a long term. However, clinical studies have shown that these three drugs have potential hepatotoxicity and can cause anti-tuberculosis drug induced liver injury (ATB-DILI) [3,4]. So far, the pathogenesis of liver injury induced by these anti-tuberculosis drugs remains unclear, and their diagnosis are usually cumbersome and difficult. Hence, there is an urgent need to develop an accurate diagnosis method to study and boost the timely treatment for ATB-DILI.

According to reports, reactive oxygen species and reactive nitrogen species (ROS and RNS) are usually produced during the process of drug-induced liver injury, which may be employed as diagnostic biomarkers to predict DILI [5–7]. Among them, peroxynitrite ($ONOO^-$) produced by the reaction of superoxide radical anion ($O_2^{\bullet-}$) and nitric oxide (NO) reflects the level of endogenous ROS and RNS, which is very suitable for early diagnosis and evaluation of DILI [8–10]. Therefore, establishing an accurate detection method for $ONOO^-$ in liver is the key to assessing liver injury.

Due to the extremely short half-life (<10 ms) and high chemical reactivity of $ONOO^-$, it is imperative to realize its direct visualization *in-situ* in biological systems [11,12]. Fluorescence imaging technology, as a non-invasive method, can monitor and image various active substances in living organisms [13–31]. Recently, several probes have been applied to systematically investigate acetaminophen (APAP, a common medicine for treating pain and fever) induced liver damage using fluorescence imaging technology [32–38]. Regardless of the recent development of fluorescent probes for detecting $ONOO^-$, there are no probes used to systematically research the liver injury mechanism of anti-tuberculosis

* Corresponding authors.
E-mail addresses: jianzhang@henu.edu.cn (J. Zhang), jmwang@henu.edu.cn (J. Wang), zhaoweili@fudan.edu.cn (W. Zhao).
[1] These authors contributed equally to this work.

https://doi.org/10.1016/j.cclet.2021.09.046
1001-8417/

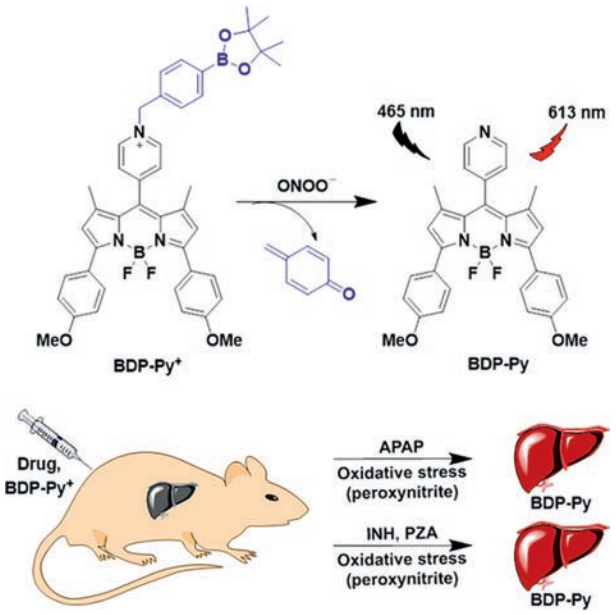

Scheme 1. Design of probe **BDP-Py⁺** to ONOO⁻.

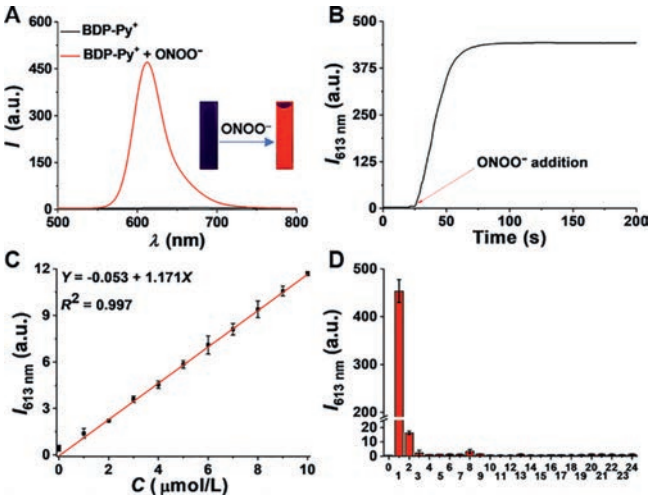

Fig. 1. Fluorescence spectral properties of **BDP-Py⁺**. (A) Fluorescence spectra of **BDP-Py⁺** (10 μmol/L) with and without ONOO⁻ (100 μmol/L). Inset: Corresponding fluorescence image under 365 nm ultraviolet radiation. (B) The reaction kinetics of **BDP-Py⁺** (10 μmol/L) reacting with ONOO⁻ (100 μmol/L). (C) Linear relationship between fluorescence intensity of **BDP-Py⁺** and ONOO⁻ concentrations. (D) Fluorescence response of **BDP-Py⁺** (10 μmol/L) to various analytes (100 μmol/L). (0) blank; (1) ONOO⁻; (2) ClO^-; (3) H_2O_2; (4) $^{\bullet}OH$; (5) $^{\bullet}O^tBu$; (6) $^1O_2$; (7) NO; (8) $O_2^{\bullet-}$; (9) TBHP; (10) K^+; (11) Na^+; (12) Mg^{2+}; (13) Cu^{2+}; (14) Zn^{2+}; (15) Fe^{2+}; (16) Fe^{3+}; (17) Al^{3+}; (18) Br^-; (19) HS^-; (20) SO_3^{2-}; (21) SO_4^{2-}; (22) Cys; (23) Hcy; (24) GSH. Conditions: PBS buffer solutions (pH 7.4, 10 mmol/L, containing 30% CH_3CN), λ_{ex} = 465 nm.

drugs [39–42]. Therefore, to realize the early diagnosis and mechanism research of anti-tuberculosis drug induced hepatotoxicity, constructing a sensitive and efficient fluorescent probe for visualizing and imaging ONOO⁻ *in vivo* is desperately needed.

To solve the above issue, we reported a small molecule probe (**BDP-Py⁺**) to investigate and image elevated ONOO⁻ level in mice liver for diagnosing DILI. In this probe, the BODIPY dye with high fluorescence quantum yield serves as the fluorophore [43–45], *p*-(bromomethyl)phenol as a self-immolative linker, and borate as the recognition group [46–48]. The hepatic ONOO⁻ oxidizes the borate group and induces self-elimination reaction, thus releasing fluorophore and detecting ONOO⁻ (Scheme 1). Thereby, **BDP-Py⁺** could detect and image ONOO⁻ *in vitro* and *in vivo* with high selectivity and sensitivity. We also utilized APAP, which had a clear mechanism of liver damage (causing liver damage through excessive oxidative stress), as a reference to study the liver damage mechanism and degree of liver damage of the first-line anti-tuberculosis drugs (rifampicin, isoniazid and pyrazinamide) through fluorescence imaging technology.

After synthesizing and characterizing the probe **BDP-Py⁺**, we first assessed its spectral properties in simulated physiological conditions (PBS buffer solutions, pH 7.4, 10 mmol/L, containing 30% CH_3CN). As shown in Fig. S1 (Supporting information) and Fig. 1A, **BDP-Py⁺** itself exhibited a maximal absorption at 580 nm and essentially no fluorescence. Density functional theory (DFT) calculations proved that **BDP-Py⁺** quenched fluorescence *via* the PET mechanism (Fig. S2 in Supporting information). After reacting with ONOO⁻, the maximum absorption peak was slightly blue-shifted to 560 nm, accompanied with an obvious color change from blue to red and a significant fluorescence enhancement (400-fold) at 613 nm. These changes were caused by peroxynitrite-induced oxidation and self-elimination reactions, which have been validated by mass spectrometry (Fig. S3 in Supporting information). Kinetic curve shown that **BDP-Py⁺** could quickly recognize ONOO⁻ within 30 s (Fig. 1B). Furthermore, the absorption spectrum of **BDP-Py⁺** slowly blue-shifted, while the fluorescence intensity at 613 nm continuously increased with increasing concentration of ONOO⁻ (0–50 μmol/L, Fig. S4 in Supporting information). More importantly, **BDP-Py⁺** displayed a satisfactory linearity with the concentration of ONOO⁻ ranging from 0 to 10 μmol/L, and the detection limit was calculated as 50 nmol/L based on $3\sigma/k$ (Fig. 1C). These results demonstrated that **BDP-Py⁺** displayed extremely high sensitivity to ONOO⁻ and could be used for the detection of trace amounts of ONOO⁻ in the biosystems. Subsequently, to exclude interference from other biologically relevant species, we conducted selectivity and anti-interference experiments. As seen in Fig. 1D and Fig. S5 (Supporting information), among many active substances, the fluorescence enhancement produced by the reaction of **BDP-Py⁺** with ONOO⁻ have an orders of magnitude advantage. Even H_2O_2, which have similar nucleophilicity and oxidization to ONOO⁻, did not lead to significant changes in fluorescence. Additionally, the pH stability experiments also proved that **BDP-Py⁺** could detect ONOO⁻ in complex physiological environments (Fig. S6 in Supporting information).

The solution tests demonstrated that **BDP-Py⁺** could achieve rapid and sensitive detection of ONOO⁻ under simulated physiological conditions, and the CCK-8 test also proved that **BDP-Py⁺** exhibited low cytotoxicity and excellent biocompatibility (Fig. S7 in Supporting information). Motivated by these results, we further evaluated the ability of probe for imaging the exogenous and endogenous ONOO⁻ in living systems. As shown in Fig. S8 (Supporting information), when RAW 264.7 cells directly incubated with SIN-1 (3-morpholinosydonimine hydrochloride, a well-known generator for ONOO⁻) and probe for 0-15 min, fluorescent signal (red) could be found within 5 min (Fig. S8 in Supporting information). Similarly, notably stronger fluorescent signal in the cells was observed after LPS and IFN-γ (lipopolysaccharide and interferon-γ can stimulate the endogenous ONOO⁻ formation) stimulation (Fig. S9 in Supporting information). The above experiments affirmed that **BDP-Py⁺** could be applied for dynamic tracking ONOO⁻ in cells.

As a verification experiment, we built DILI model cells to study the ability of **BDP-Py⁺** imaging and evaluating drug-induced hepatotoxicity. According to previous reports [34,41], overdose of APAP might cause liver damage through excessive oxidative stress, during which large amounts of ROS and RNS (including ONOO⁻) were produced. Employing the probe, we monitored the alteration of

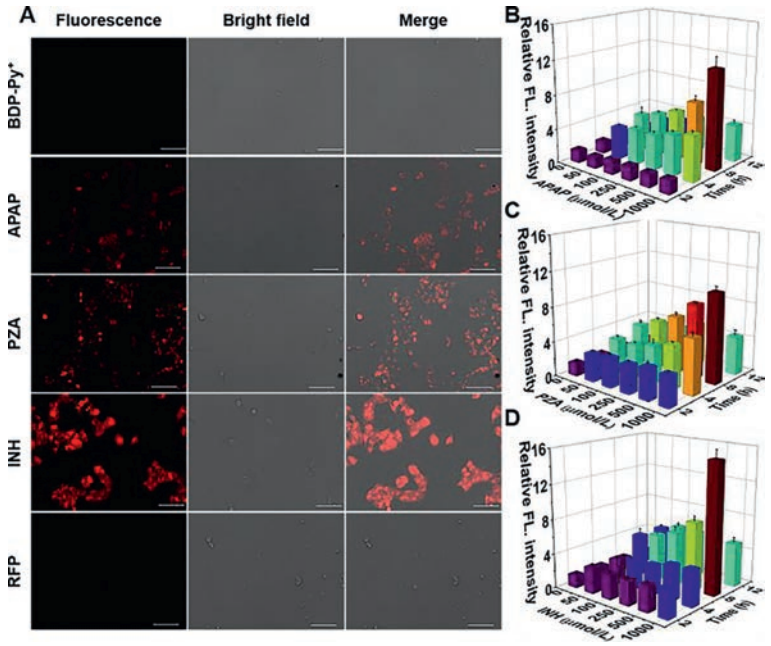

Fig. 2. Fluorescence images of liver injury induced by different drugs in HepG2 cells. (A) First line: The cells were treated with **BDP-Py⁺** (10 μmol/L). Second through fifth lines: The cells were pretreated with different drugs (APAP, PZA, INH, and RFP, 1 mmol/L) for 8 h, and then treated with **BDP-Py⁺** (10 μmol/L) for 10 min. (B-D) Drugs (APAP, PZA, and INH) affected change in fluorescence intensity in dose- and time-dependent manners in HepG2 cells. λ_{ex} = 530–570 nm, λ_{em} = 575–640 nm. Scale bar: 100 μm.

$ONOO^-$ in the DILI model constructed by APAP. Through fluorescence imaging, with the increase of APAP concentration (0–1000 μmol/L) and the extension of the medication time (0–8 h), the fluorescence of the red channel gradually increased (Figs. S10 and S11 in Supporting information). Overall, APAP treated HepG2 cells revealed a dose- and time-dependent fluorescence enhancement (Fig. S12 in Supporting information). This probe not only captured and displayed liver damage caused by a small amount of APAP in a short period of time, but also can track $ONOO^-$ caused by APAP in real time for a long time. As shown in Fig. S12, at 4 h after cells being treated with APAP, the obvious fluorescence was observed, with more strong fluorescence signal visible after 8 h. However, a weaker fluorescence signal was observed at 12 h, which may be because $ONOO^-$ produced in cells was metabolized by the cells. Taken together, these results implied that **BDP-Py⁺** could accurately monitor the changes in intracellular $ONOO^-$ levels during APAP-induced liver injury.

With the support of these data, then we investigated the evaluation function of **BDP-Py⁺** on the hepatotoxicity induced by anti-tuberculosis drugs. The first-line anti-tuberculosis drugs, such as PZA, INH, and RFP, all have potential hepatotoxicity, however, the precise mechanisms of this toxicity are unclear. In following works, we took advantage of these drugs to construct liver injury models, and further applied **BDP-Py⁺** to monitor the changes of $ONOO^-$ concentration when anti-tuberculosis drugs induced liver injury and to explore possible damage mechanisms. As shown in Fig. 2A, after stimulation with overdose, significant fluorescence signals were observed in the HepG2 cells incubated with APAP, PZA, and INH, whereas the HepG2 cells incubated with RFP did not show any noticeable fluorescence signal. The fluorescence behaviors caused by these drugs were consistent in HL-7702 cells (Fig. S13 in Supporting information). Through DHE (dihydroethidium) staining, we found that APAP, PZA, and INH could induce cells to produce ROS, while RFP could not cause oxidative burst (Fig. S14 in Supporting information). These outcomes demonstrated that the liver damage mechanisms of PZA and INH were the same as APAP, and these drugs could induce the overproduction of $ONOO^-$ through oxidative stress to cause hepatic damage. However, RFP induced liver damage through other mechanism than oxidative stress. Meanwhile, we also verified that PZA and INH could induce the activation of fluorescence in dose- and time-dependent manners in living cells (Figs. S15-S20 in Supporting information). The results in Figs. 2B-D more clearly showed the dose-effect and time-effect relationships of APAP, PZA, and INH induced liver injury.

To attest the potential application of **BDP-Py⁺** *in vivo*, we first evaluated whether it could sensitively and efficiently realize fluorescence imaging of $ONOO^-$ in mice. All animal care and experimental protocols for this study were approved by the Animal Experiment Ethics Committee of Henan University (Reference number: HUSOM2017-167). The $ONOO^-$ was produced *in vivo* through acute inflammation induced by LPS in the tibiotarsal joints of mice. In the mouse model of leg joint inflammation (right leg), the fluorescence signal intensity gradually increased over time and reached a plateau within 60 min (Fig. S21 in Supporting information). At this time, the fluorescence intensity was still 2.2-fold that of the control group (left leg). The results showed that **BDP-Py⁺** could be exploited for real-time detection and imaging of $ONOO^-$ *in vivo*.

Inspired by the findings above, we utilized the drugs-induced mice liver injury models and **BDP-Py⁺** to investigate the ATB-DILI mechanisms and evaluate the degrees of hepatic injury of different drugs *in vivo*. To achieve this goal, dose- and time-dependent experiments were performed. After the administration, the main organs of the mice were dissected for fluorescence imaging. Compared with the control group, the groups pretreated with APAP exhibited stronger fluorescence signal, and higher dose of APAP produced more outstanding fluorescence (Figs. 3A and B). In this study, we found that obvious fluorescent signal could be captured after 12 h treated with 100 mg/kg APAP and 4 h treated with 300 mg/kg APAP, and liver damage induced by APAP aggravated over time (0−12 h, Fig. S22). After 24 h of administration, the decreased in fluorescence intensity may be due to the metabolism of $ONOO^-$ (Fig. S22). Clinically, hepatic injury can be diagnosed by analyzing the changes in levels of serum enzymes including AST (aspartate transaminase), and ALT (alanine transaminase). Therefore, we additionally examined the levels of these enzymes in the serum of

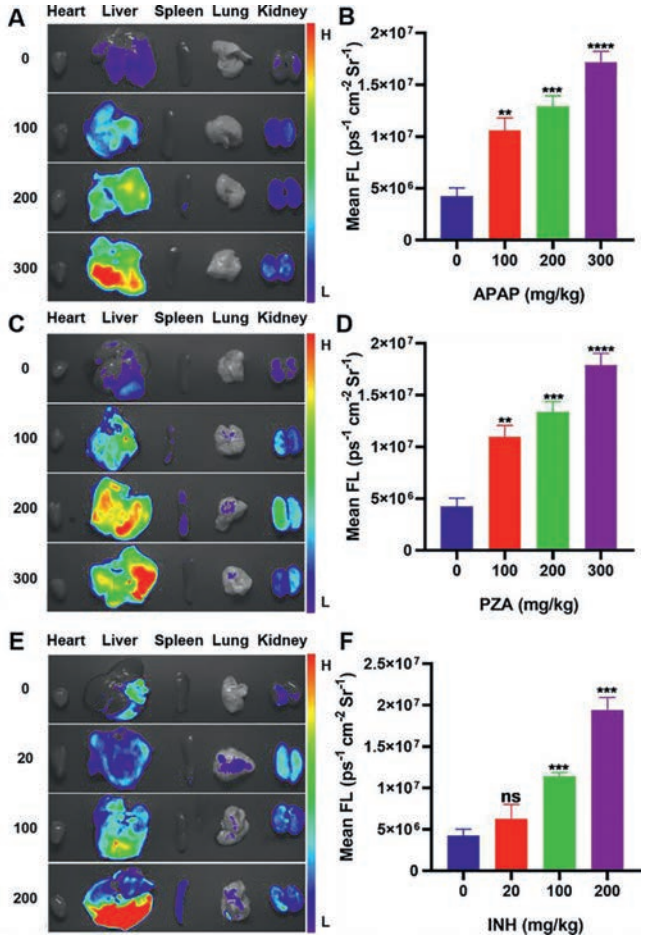

Fig. 3. Fluorescence images of mice organs treated with various concentrations of (A) APAP (0, 100, 200, 300 mg/kg for 12 h), (C) PZA (0, 100, 200, 300 mg/kg for 12 h), and (E) INH (0, 20, 100, 200 mg/kg for 8 h), respectively. (B, D, F) Fluorescence intensities of A, C, E. Statistical analysis was performed with a two-tailed Student's t-test. ** $P < 0.01$, *** $P < 0.001$, **** $P < 0.0001$, n.s. denotes no significant difference. λ_{ex} = 540–580 nm, λ_{em} = 590–670 nm.

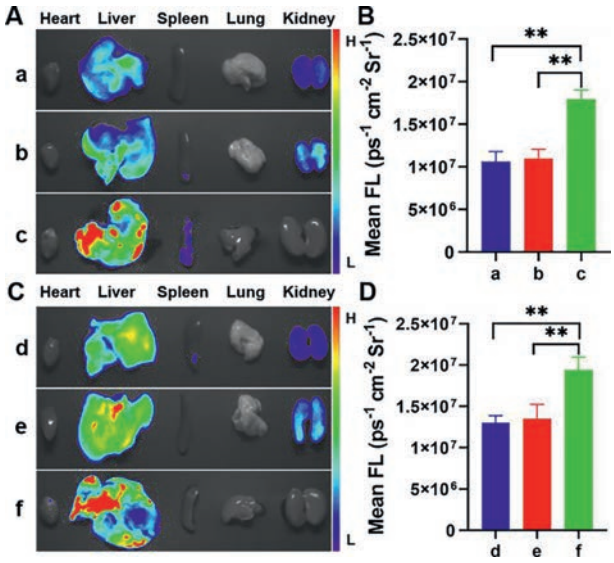

Fig. 4. Fluorescence images of mice organs induced by different drugs. (A) Fluorescence images of mice treated with 100 mg/kg (a) APAP, (b) PZA, and (c) INH for 12 h, respectively. (B) Fluorescence intensities of a-c. (C) Fluorescence images of mice treated with 200 mg/kg (d) APAP, (e) PZA for 12 h, and (f) INH for 8 h, respectively. (D) Fluorescence intensities of d-f. Statistical analysis was performed with a two-tailed Student's t-test. ** $P < 0.01$. λ_{ex} = 530–570 nm, λ_{em} = 575–640 nm.

mice. These liver damage indicators were not significantly, regularly and reliably up-regulated in dose- and time-dependent experiments (Figs. S23 and S24 in Supporting information) demonstrated that these enzymatic biomarkers were ineffective in the diagnosis of early liver injury. Besides, the liver tissue sections of mice stained with hematoxylin and eosin (H&E) demonstrated that APAP caused damage and necrosis of the liver after 12 h treated with 200 mg/kg APAP and 8 h treated with 300 mg/kg APAP, the degrees of damage were aggravated with increasing dose and time (Figs. S25 and S26 in Supporting information). Comparing with the serum enzymes detection and H&E staining, the results indicated that **BDP-Py$^+$** could monitor the up-regulation of $ONOO^-$ levels to achieve early diagnosis of DILI before solid lesions in liver.

Based on the above studies, we also explored the liver injury models induced by PZA and INH. Fortunately, PZA-induced liver injury also had similar dose- and time-dependent effects (Figs. 3C and D, Fig. S27 in Supporting information). It is worth noting that INH produced more serious liver damage. When higher doses of INH (300 mg/kg and 200 mg/kg) were intraperitoneally injected into mice, they died within 2 h and 12 h, respectively. After adjusting doses, the significant dose- and time-dependent relationships could still be observed in INH-induced acute liver injury models, with five-fold fluorescence enhancement for the highest dose compared with the control group (Figs. 3E and F, Fig. S28 in Supporting information). In consequence, **BDP-Py$^+$** could not only be applied to explore the liver injury mechanism of anti-tuberculosis drugs, but also to verify the dose-effect and time-effect relationships of these drugs.

In order to fully confirm that the hepatotoxicity of INH was more severe than that of PZA and APAP, we investigated the degrees of liver damage induced by the three drugs in the same dose and the same time. As shown in Figs. 4A and B, significantly much higher fluorescence intensity was observed in the liver of INH-treated mice than PZA and APAP-treated mice. Remarkably, at the same dose, compared with pyrazinamide and APAP, mice treated with INH exhibited much stronger fluorescence in a shorter period of time (Figs. 4C and D). It can be seen that the liver toxicity caused by INH was significantly stronger than that of PZA and APAP. These data indicated that **BDP-Py$^+$** could serve as a promising tool for screening out and evaluating the hepatotoxicity of different drugs by detecting and imaging $ONOO^-$.

In summary, we designed and synthesized a BODIPY-based fluorescent probe **BDP-Py$^+$** for rapid, sensitive and efficient detection of $ONOO^-$. Applying **BDP-Py$^+$**, we realized the diagnosis and mechanism research of anti-tuberculosis drug-induced liver injury. Using APAP as a reference, we verified that the anti-tuberculosis drugs PZA and INH also produced $ONOO^-$ through oxidative stress to cause liver damage, while RFP *via* other mechanism. In addition, **BDP-Py$^+$** could be applied to screen out and evaluate the hepatotoxicity of different drugs. Comparing with the serum enzymes detection and H&E staining, the probe could monitor the up-regulation of $ONOO^-$ levels to achieve early diagnosis of DILI before solid lesions in liver. Collectively, this work provided a favorable tool for the diagnosis of DILI, exploring the mechanism of DILI, and assessing the degree of drug-induced liver injury.

Declaration of competing interest

The authors declare that they have no known competing financial interests or personal relationships that could have appeared to influence the work reported in this paper.

Acknowledgments

This research was financially supported by the National Natural Science Foundation of China (Nos. 82030107 and 21702046), the China Postdoctoral Science Foundation (No. 2018M632757), the Key Scientific and Technological Project of Henan Province (Nos. 212102311064 and 212102310870) and the Innovation Scientists and Technicians Troop Construction Projects of Henan Province (No. 20IRTSTHN020).

Supplementary materials

Supplementary material associated with this article can be found, in the online version, at doi:10.1016/j.cclet.2021.09.046.

References

[1] W.M. Lee, Clin. Liver Dis. 17 (2013) 575–586.
[2] M. Pieroni, D. Machado, E. Azzali, et al., J. Med. Chem. 58 (2015) 5842–5853.
[3] J.Y. Wang, C.H. Tsai, Y.L. Lee, et al., Medicine 94 (2015) 982.
[4] T. Haque, E. Sasatomi, P.H. Hayashi, Gut Liver 10 (2016) 27–36.
[5] A.J. Shuhendler, K. Pu, L. Cui, J.P. Uetrecht, J. Rao, Nat. Biotechnol. 32 (2014) 373–380.
[6] W.M. Lee, J. Hepatol. 67 (2017) 1324–1331.
[7] C. Szabo, H. Ischiropoulos, R. Radi, Nat. Rev. Drug Discov. 6 (2007) 662–680.
[8] P. Pacher, J.S. Beckman, L. Liaudet, Physiol. Rev. 87 (2007) 315–424.
[9] G. Ferrer-Sueta, R. Radi, ACS Chem. Biol. 4 (2009) 161–177.
[10] R.J. Radi, Biol. Chem. 288 (2013) 26464–26472.
[11] N. Ieda, H. Nakagawa, T. Peng, et al., J. Am. Chem. Soc. 134 (2012) 2563–2568.
[12] C. Ducrocq, B. Blanchard, B. Pignatelli, H. Ohshima, Cell. Mol. Life Sci. 55 (1999) 1068–1077.
[13] G. Yin, T. Niu, T. Yu, et al., Angew. Chem. Int. Ed. 58 (2019) 4557–4561.
[14] Y. Gan, G. Yin, T. Yu, et al., Talanta 210 (2020) 120612.
[15] H. Li, Q. Yao, F. Xu, et al., Angew. Chem. Int. Ed. 59 (2020) 10186–10195.
[16] V. Nguyen, Y. Yim, S. Kim, et al., Angew. Chem. Int. Ed. 59 (2020) 8957–8962.
[17] P. Chen, H. Zhang, L. Niu, et al., Adv. Funct. Mater. 27 (2017) 1700332.
[18] N. Liu, P. Chen, J. Wang, L. Niu, Q. Yang, Chin. Chem. Lett. 30 (2019) 1939–1941.
[19] P. Lu, X. Zhang, T. Ren, L. Yuan, Chin. Chem. Lett. 31 (2020) 2980–2984.
[20] K. Wang, W. Ma, Y. Xu, et al., Chin. Chem. Lett. 31 (2020) 3149–3152.
[21] J. Han, X. Yue, J. Wang, et al., Chin. Chem. Lett. 31 (2020) 1508–1510.
[22] X. Ren, L. Liao, Z. Yang, et al., Chin. Chem. Lett. 32 (2021) 1061–1065.
[23] J. Zhang, N. Wang, X. Ji, et al., Chem. Eur. J. 26 (2020) 4172–4192.
[24] D. Shi, S. Chen, B. Dong, et al., Chem. Sci. 10 (2019) 3715–3722.
[25] Y. Zhang, Y.Gao H.Teng, et al., Chin. Chem. Lett. 31 (2020) 2917–2920.
[26] H. Teng, J. Tian, D. Sun, et al., Sens. Actuat. B: Chem. 319 (2020) 128288.
[27] B. Chen, S. Mao, Y. Sun, et al., Chem. Commun. 57 (2021) 4376–4379.
[28] J. Zhang, J. Kan, Y. Sun, et al., ACS Appl. Bio. Mater. 4 (2021) 2080–2088.
[29] J. Zhou, P. Jangili, S. Son, et al., Adv. Mater. 32 (2020) 2001945.
[30] C. Zhang, H. Xie, T. Zhan, et al., Chem. Commun. 55 (2019) 9444–9447.
[31] B. Chen, C. Li, J. Zhang, et al., Chem. Commun. 55 (2019) 7410–7413.
[32] D. Cheng, W. Xu, X. Gong, L. Yuan, X. Zhang, Acc. Chem. Res. 54 (2021) 403–415.
[33] Y. Huang, Y. Qi, C. Zhan, F. Zeng, S. Wu, Anal. Chem. 91 (2019) 8085–8092.
[34] D. Cheng, J. Peng, Y. Lv, et al., J. Am. Chem. Soc. 141 (2019) 6352–6361.
[35] W. Jiang, Y. Li, W. Wang, et al., Chem. Commun. 55 (2019) 14307–14310.
[36] L. Wu, Q. Ding, X. Wang, et al., Anal. Chem. 92 (2020) 1245–1251.
[37] H. Wang, C. Liu, Z. He, et al., Anal. Chem. 93 (2021) 6551–6558.
[38] L. Wu, J. Liu, X. Tian, et al., Chem. Sci. 12 (2021) 3921–3928.
[39] B. Wang, Y. Wang, Y. Wang, et al., Anal. Chem. 92 (2020) 4154–4163.
[40] D. Cheng, Y. Pan, L. Wang, et al., J. Am. Chem. Soc. 139 (2017) 285–292.
[41] D. Cheng, W. Xu, L. Yuan, X. Zhang, Anal. Chem. 89 (2017) 7693–7700.
[42] J. Chen, D. Huang, M. She, et al., ACS Sens. 6 (2021) 628–640.
[43] X. Ji, N. Wang, J. Zhang, et al., Dyes Pigments 187 (2021) 109089.
[44] N. Wang, M. Chen, J. Gao, et al., Talanta 195 (2019) 281–289.
[45] J. Zhang, X. Ji, J. Zhou, et al., Sens. Actuat. B: Chem. 257 (2018) 1076–1082.
[46] A.C. Sedgwick, H.H. Han, J.E. Gardiner, et al., Chem. Sci. 9 (2018) 3672–3676.
[47] S. Palanisamy, P.Y. Wu, S.C. Wu, et al., Biosens. Bioelectron. 91 (2017) 849–856.
[48] M. Weber, H.H. Han, B.H. Li, et al., Chem. Sci. 11 (2020) 8567–8571.